6) *Weyl, W. A.* and *W. C. Ormsby*, in: Rheology. Ed. by *F. R. Eirich*, Vol. 3, Chap. 7 (New York 1960).
7) *Freundlich, H.*, Actualities Sci. et ind. No. 267 (1935).
8) *von Engelhardt*, Kolloid-Z. **102**, 217 (1943).
9) *Hauser, E. A.*, Chem. Rev. **37**, 287 (1945).
10) *Usher, F. L.*, Proc. Roy. Soc. **A 125**, 143 (1929). *McDowell, C. M.* and *F. L. Usher*, Proc. Roy. Soc. **A 131**, 564 (1931).
11) *Kuhn, W. Z.*, Z. physik chem. (Leipzig) **A 161**, 564 (1931). *Hauser, E. A.* and *C. E. Reed*, J. Phys. Chem. **40**, 1169 (1936); **41**, 911 (1937).
12) *Hofmann, U.*, Kolloid-Z. **125**, 86 (1952).
13) *Macey, H. H.*, Trans. Brit. Ceram. Soc. **43**, 5, (1944). **41**, 73 (1942).
14) *McBain, J. W.*, J. Phys. Chem. **30**, 239 (1926).
15) *Grim, R. E.* and *F. L. Cuthbert*, J. Amer. Ceram. Soc. **28**, 90 (1945).
16) *Payne, A. R.* and *J. A. C. Harwood*, J. Appl. Polymer Sci. **12**, 889 (1968).
17) *Grosch, K. A.*, J. Appl. Polymer Sci. **12**, 915 (1968).
18) *Westlinning, H., G. Butenuth* and *G. Leine-Weber*, Makromol. Chemie **50**, 253 (1961).
19) *Payne, A. R.*, J. Colloid Sci. **19**, 744 (1964).
20) *Payne, A. R.*, J. Appl. Polymer Sci. **2**, 383 (1962).

Authors' address:
A. R. Payne and *R. E. Whittaker*
Shoe and Allied Trades
Research Association, Satra House, Kettering (England)

Appendix

Compounding details

RSS (SMR 5)	100
Zinc Oxide	5
Stearic Acid	2
Sulphur	2.5
CBS	0.6

The above gum mix with:
40, 80, 120, 160, 200, 240 pph Bentonite clay
and also with:
40, 80, 120, 160, 200, 240, 280 pph Stockalite clay.
All cured for 40 minutes at 140 °C.

Koninklijke Shell-Laboratorium, Shell Research N. V. Amsterdam (Netherlands)

The dynamic shear modulus of bitumens as a function of frequency and temperature

By R. Jongepier and B. Kuilman

With 7 figures in 12 details and 2 tables

(Received January 18, 1969)

1. Introduction

Bitumens are viscoelastic liquids prepared from crude oil distillation residues. They include members with widely varying properties, satisfying the requirements of a multitude of applications. Among these the rheological properties are usually considered of paramount importance.

The bitumen rheologist has to deal with the linear as well as the non-linear behaviour of his materials.

In the present paper we shall confine our attention to the linear visoelastic properties as a function of frequency and temperature. These properties have their bearing not only on the design of road constructions as far as road bitumens are concerned, but they also enable many other bitumens to be characterized.

By a very useful graphical representation *Van der Poel* (1) demonstrated the regular pattern of the thermorheological properties of bitumens using routine test data for the characterization of type and hardness.

Brodnyan (2) gives a comparable survey of a wide range of types of bitumen and discusses the influence of frequency and temperature separately. He applied a "free volume" equation to account for the effects of temperature.

The free volume concept has been further explored for bitumens by other investigators (3, 4), who combined dilatometric glass-transition temperature with thermorheological measurements.

The regular patterns for the frequency dependence in ref. (1) and (2) suggest that bitumens can be described by a common formula and the observations in ref. (3) and (4) lead to the same conclusion for the influence of temperature. The information in the literature is, however, not sufficient to establish both formulas as well as their mutual relation and the significance of glass-transition temperatures in this respect. Hence we investigated the thermorheological properties and glass-transition temperatures of a series of bitumens of varying types.

2. Experimental

The sample collection consisted of three groups of bitumens:

(a) "Pitch-type" bitumens, which are known as strongly temperature-susceptible: samples 1 and 2.

(b) "Road bitumens", which are used as binders in bituminous mixes for road building and in hydraulic applications. This group has moderate temperature susceptibility: samples 3–10.

(c) The samples 11–14 are "blown type bitumens" or "rubbery grades", which have been processed to impart low temperature susceptibility. Samples 11–13 represent moderate examples of this group, whereas no. 14 is an extreme case. These bitumens are used in industrial applications such as coating, impregnation or roofing materials.

Often, reference is made to the colloid-chemical structure of the various bitumens, group (a) representing the sol type, group (b) medium and group (c) gel-type bitumens.

The newtonian (shear-rate independent) viscosities were measured with dark-oil viscometers (5) or, if some shear rate dependence was expected, with an Epprecht Rheomat 15; both instruments covered the range from 1 to 1000 P.

The range from 100 to 10^7 P was measured with a *Weissenberg* R 16 rheogoniometer, fitted with a 4°, 2.5 cm cone and plate. The temperature of the sample was controlled by the standard electrical heating outfit.

The dynamic modulus measurements above room temperature were made with the same instrument. Below room temperature we used Labout's micro-elastometer (6). Our most recent measurements (samples 1, 2, 8, 13 and 14) were made with a *Weissenberg* R 17 rheogoniometer, which was equipped with a "fluid circulation chamber" temperature control. With this set-up moduli could also be measured below room temperature. For the moduli below 10^8 dyn/cm² we again used a 4°, 2.5 cm cone and plate, but for the higher moduli 1-cm diameter parallel plates, whose distance was adjusted so as to keep the stiffness of the sample low with respect to the stiffness of the rheogoniometer. A gap of 1 cm was sufficient for measurements of the glass moduli (5×10^9 dyn/cm²). Brittle fracture of the sample determined the lowest test temperatures. The R 17 rheogoniometer was fitted with Sanborn type 7 DCDT-100 transducers and the solid state electronic measuring circuits (made in our laboratory) were provided with active filters. The dynamic measurements were corrected for movement and inertia of the torsion head and converted to dynamic modulus and phase angle by a computer programme.

Glass transition temperatures were determined by volume dilatometry according to a method which *Schmidt* proposed for bitumens (7). We used Rhodorsil 41 V 10 silicone fluid as the confining liquid, which, unlike methanol, gave virtually no interaction with bitumens (especially blown bitumens). The junction between the bottom flange of the capillary and the top flange of the cup was sealed with a flat ring of 0.3 mm thick polyethylene foil. The calibrated capillary was surrounded by a glass air jacket, which ensured uniform room temperature along the capillary. For the blown samples we could not use the sample preparation proposed by *Schmidt* (7) but slightly tapering, nearly cylindrical samples were made by using Teflon moulds instead of brass ones. Finally we altered the filling procedure. Instead of adding the confining liquid through a long hypodermic syringe needle, we placed the flange of the capillary on top of the cup with the confining liquid gently flowing down the capillary. This was found to be a quick and trouble-free procedure to fill the dilatometer without air bubbles being formed.

The dilatometric measurements were made at a cooling rate of 1 °C/min and the readings were corrected for contraction of the cup and for the temperature difference between capillary and cup.

3. Results

As a typical example of the thermorheological results we plotted the data obtained with sample no. 8. We chose the modulus-phase angle form of notation and both modulus $|G(\omega)|$ and circular frequency (ω) scales were taken logarithmically. For compactness of representation the measured viscosities $\eta_0(T)$ were also plotted as moduli by using

$$|G(\omega)| = \eta_0(T)\,\omega, \qquad [1]$$

which is valid at temperatures above 40 °C for the frequency interval of our measurements.

Fig. 1 exhibits "thermorheological simplicity" (8): The frequency-temperature superposition possible with such a material, is generally effected after applying a small correction factor to moduli and viscosities. Most investigators apply the reduced variables given in (9), which derive from the

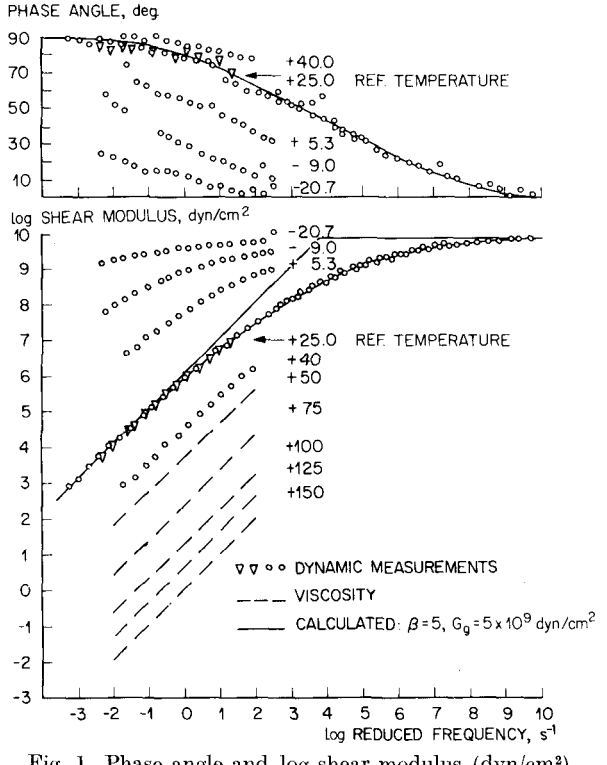

Fig. 1. Phase angle and log shear modulus (dyn/cm²), temperature (°C) versus log reduced frequency; sample No. 8

entropy spring nature of viscoelasticity. On the other hand, one can use a correction factor based on the measured temperature dependence of the glassy modulus (10).

In principle, different corrections lead to different results of the frequency-temperature superposition. However, a correction which is drastically wrong will betray itself by the impossibility of applying frequency-temperature superposition to the "corrected" moduli.

The lack of knowledge of the temperature dependence of the glassy moduli of bitumens induced us to use the reduced variables given in *Ferry*'s book (9). The other moduli and viscosities in this work have all been reduced to 20 °C.

Fig. 1 gives the master curve of the reduced dynamic modulus of sample no. 8 obtained from frequency-temperature superposition.

Each modulus value at its new position of reduced frequency has a corresponding phase angle value; hence we can obtain at the same time a master curve of phase angle against reduced frequency. The latter corresponds with circular frequency at 25 °C for the case of fig. 1.

The results in fig. 1 typically represent road bitumens; in fig. 2 we plotted the master curve of a pitch-type bitumen and of the extreme rubbery type-bitumen, samples 1 and 14, respectively. In this figure the frequency has been replaced by a (dimensionless) relative frequency ω_r:

$$\omega_r = \frac{\omega \eta_0}{G_g}, \qquad [2]$$

under discussion do not vary measurably with the type of bitumen, plots of modulus in which G_g represents the glassy modulus. As the glass moduli at the temperatures against ω_r have coincident viscous flow and elastic deformation asymptotes and the frequency is taken relative to the intersection point of the asymptotes. The frequency at the intersection point corresponds with the reciprocal relaxation time of a Maxwell body and for comparison we have also shown the curves for such a material with only one relaxation time.

Besides the master curves in fig. 1 and 2, representing the effect of frequency at constant temperature, our experimental data

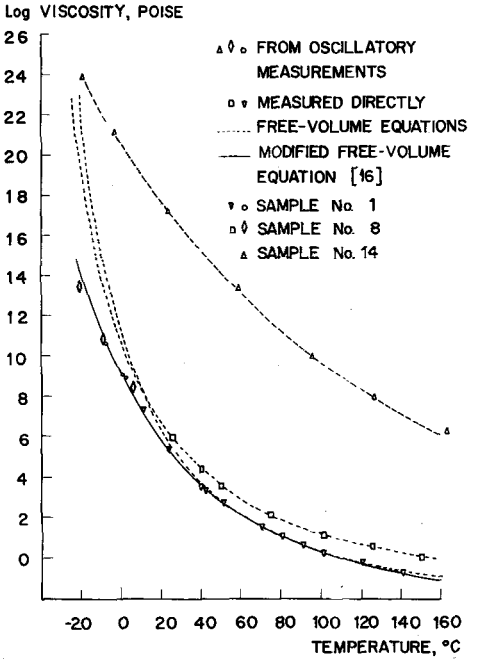

Fig. 3. Log viscosity (P) versus temperature (°C)

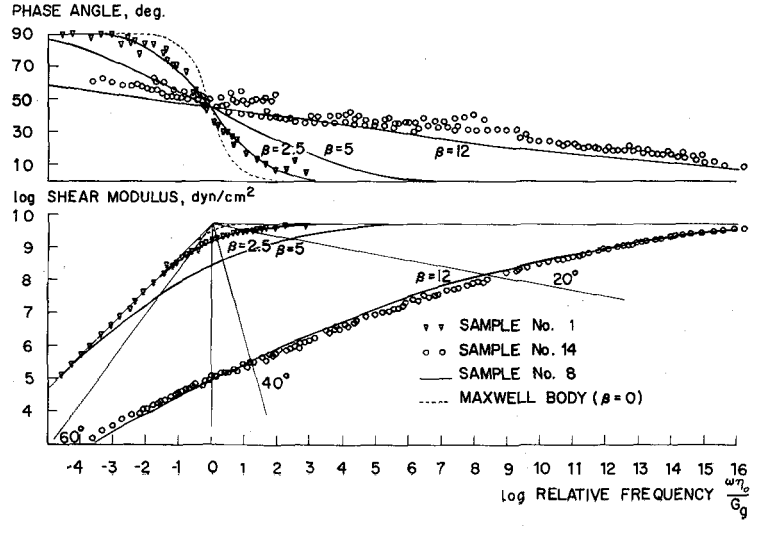

Fig. 2. Phase angle and log shear modulus (dyn/cm²) versus log relative frequency

also give the effect of temperature alone, viz. the frequency-temperature shifts.

Samples 8 and 1 in fig. 1 and 2 provided measured viscosity values as well as calculated values from viscous flow asymptotes. These enabled us to plot the frequency-temperature curves as viscosity-temperature functions (see fig. 3).

Sample 14, however, provided neither reliable zero shear viscosity data nor modulus data on a viscous flow asymptote. The position of the viscous flow asymptote at a given temperature, defining the viscosity at that temperature, was estimated from an assumed form of the master curve, which assumption is discussed in the next section. The frequency-temperature shifts have been plotted as viscosity-temperature data on the basis of this estimate. The uncertainty in the viscosity of sample 14 only causes an uncertainty in the vertical position of the curve of this sample in fig. 3, but not in its shape.

The results obtained with all the other samples are presented in a numerical form, which will be discussed in the next section.

Fig. 4 shows an example of the dilatometric results (sample no. 3). The results obtained with the other samples – glass-transition temperatures and the coefficients of expansion from the liquid branch (a) and the glassy branch (b) – are collected in table 1.

Table 1

Sample	T_g [1]	α_1 [2]	α_g [3]	C_1 [4]	C_2 [4]	f_g [5]
1	−25	5.6	2.7	36.3	19.0	0.6
2	−33	5.8	3.1	29.6	25.0	0.7
3	−38	6.5	3.3	22.9	38.0	1.2
4	−48	6.3	3.3	54.5	15.0	0.5
5	−39	5.9	3.0	36.9	27.0	0.8
6	−32	5.9	3.0	27.4	32.0	0.9
7	−43	6.2	3.0	30.5	32.0	1.0
8	−34	6.1	3.2	41.5	18.0	0.5
9	−34	5.8	3.1	29.0	28.0	0.8
10	−40	6.6	3.5	49.8	12.0	0.4
11	−33	6.4	3.3	30.0	80.0	2.5
12	−43	6.8	3.6	40.7	55.0	1.8
13	−40	6.0	2.8	33.1	86.0	2.8
14	−34	5.7	3.0	41.1	188.0	5.1

Remarks

[1]) Dilatometric glass-transition temperature, °C estimated max. error ± 3 °C.

[2]) Coefficient of expansion ($°C^{-1}$) × 10^4 (liq. state) estimated max. error ± 5%.

[3]) Coefficient of expansion ($°C^{-1}$) × 10^4 (glassy state) estimated max. error ± 5%.

[4]) WLF constants with T_g as a reference.

[5]) Percentage free volume at T_g.

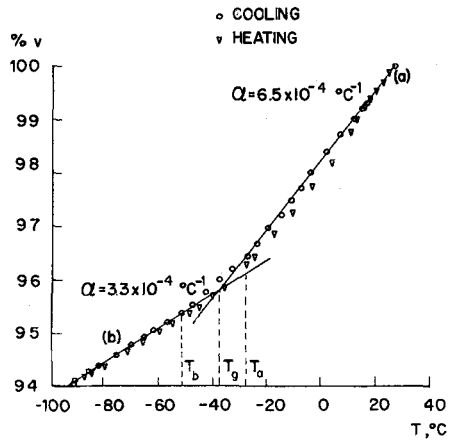

Fig. 4. Dilatometric curve of sample No. 3 at a cooling (heating) rate of 1 °C/min

4. Discussion

Before considering details of the curves obtained by frequency-temperature superposition the following has to be noted.

Frequency-temperature superposition is – in its generality – only qualitatively understood. Hence, the modulus values obtained as a function of reduced frequency should be checked against measurements at real frequencies, equal to some reduced frequencies before a master curve can be read as a modulus curve against real frequency at the reference temperature. Such checks have been made by *Brodnyan* (2) on bitumen. When these checks are impossible, the superposition of frequency and temperature should be considered as an artefact, which is at least the best approximation for the modulus function outside the frequency range studied. It is, however, certainly the most favourable means of separating the influence of frequency and of temperature on thermorheologically simple materials.

We will first discuss the shape of the master curves in fig. 1 and 2. It was found that this shape can be represented by two characteristic numbers, which will be given for the remaining samples. Then we will consider the viscosity-temperature curves and express these by free-volume parameters. We will finally discuss the dependence of both sets of parameters on the type of bitumen and the role played by the glass-transition temperature.

a) Master curves

Rather than analysing the frequency dependence of the dynamic moduli we

analyse the relaxation spectra underlying the curves in fig. 1 and 2. *R. N. Saal* (11) observed that bitumens can be described by relaxation spectra based on a Gaussian distribution of log relaxation time. We have confirmed this by an analysis according to *Ninomya* and *Ferry* (12) of some recently measured master curves. This spectrum is defined by three factors: a width parameter β, a time constant τ_m, which determines the position of the spectrum along the relaxation time or τ axis at a given temperature, and finally the glassy modulus G_g, which defines the magnitude of the contributions of various relaxation times to the moduli. The "logarithmic" relaxation time distribution of the "log normal" type is now given by:

$$H(\tau) = \frac{G_g}{\beta\sqrt{\pi}} \exp - \left\{\frac{\ln \tau/\tau_m}{\beta}\right\}^2. \qquad [3]$$

The glassy modulus is defined by:

$$G_g = \int_{-\infty}^{\infty} H(\tau)\, d \ln \tau \qquad [4]$$

and the viscosity η_0 follows from eq. [3] by:

$$\eta_0 = \int_{-\infty}^{\infty} H(\tau)\, \tau\, d \ln \tau = G_g\, \tau_m \exp \frac{\beta^2}{4}. \qquad [5]$$

The storage and loss moduli are expressed by eq. [7] and [8] after the following substitutions:

$$u = \ln \omega\tau \quad \text{and} \quad x = \frac{2}{\beta^2} \ln \omega_r: \qquad [6]$$

$$G_1(x) = \frac{G_g}{\beta\sqrt{\pi}} \exp - \left\{\frac{\beta\,(x - \tfrac{1}{2})}{2}\right\}^2 \times \int_0^{\infty} \exp - \left(\frac{u}{\beta}\right)^2 \frac{\cosh\,(x + \tfrac{1}{2})\, u}{\cosh u}\, du \qquad [7]$$

$$G_2(x) = \frac{G_g}{\beta\sqrt{\pi}} \exp - \left\{\frac{\beta\,(x - \tfrac{1}{2})}{2}\right\}^2 \times \int_0^{\infty} \exp - \left(\frac{u}{\beta}\right)^2 \frac{\cosh\,(x - \tfrac{1}{2})\, u}{\cosh u}\, du. \qquad [8]$$

It is seen from eq. [7] and [8] that $x = 0$ (or $\omega_r = 1$) constitutes a symmetry point for which the phase angle $\varphi\,(x)$ is equal to $\pi/4$ and

$$\tan \varphi\,(x) = \cot \varphi\,(-x). \qquad [9]$$

while we deduce for the corresponding moduli:

$$\frac{|G(x)|}{G_g} = \frac{|G(-x)|}{|G(-x)|_{\text{visc}}}, \qquad [10]$$

in which the numerator of the right-hand member is the modulus value on the viscous flow asymptote (eq. [1]) for the given x or relative frequency.

In order to check the log normal spectra and to evaluate the width parameter β for each sample, eq. [7] and [8] have to be integrated. This can only be performed numerically, as done before (13, 14). The numerical data in the literature, however, did not cover a sufficiently wide range of β values; hence we computed the integrals again and converted the results into modulus and phase angle values. The values of β were obtained by selection of the calculated master curve pair (modulus and phase angle) which fitted the experimental results best.

The curves in fig. 1 and 2 correspond with calculated curves for the β values listed in table 2. The curve for a *Maxwell* body in fig. 2 constitutes a limiting case for β approaching zero. In general, the calculated curves fitted the experimental data within the experimental error. The experimental scatter was largest with samples 11–14 ($\beta > 6$). These rubbery materials showed more tendency to give unrepeatable results than did the other types. This is presumably due to ageing phenomena during sample preparation. Besides, with these rubbery materials the bulk of the measurements gave low moduli, which could only be measured at shear amplitudes of the order of 0.4, whereas the other samples could be measured at amplitudes of 0.1. As a consequence, there may have been more influence of non-linearity in the tests on samples 11–14 than in the other samples. However, in all cases the stress signal traces were sinusoidal.

With the high-β samples newtonian viscosity values cannot be measured directly. Neither can we obtain newtonian viscosities from measured viscosity-shear rate functions, owing to the lack of a reliable extrapolation to zero shear rate. Table 2 gives the viscosities at 20 °C as derived from the best fitting calculated master curves. For the low-β samples, we also give the values from actual viscosity measurements at higher temperatures after extrapolation to 20 °C by the free-volume type viscosity-temperature relations discussed below. The agreement is sufficient for normal bitumen practice. By means of eq. [5] we calculated the midpoint value τ_m of the spectra at 20 °C. In this calculation we took $G_g = 5 \times 10^9$ dyn/cm^2 for all bitumens, as this value applies to all our measurements. It is interesting to note

Table 2

Sample	β[1]	log η_{dyn}[2]	log η_{visc}[3]	log τ_m[4]	B[5]	T_0[6]	A[7]
1	2.5	5.8	6.4	— 4.6	690	229	— 5.0
2	4.0	5.2	5.1	— 6.2	739	215	— 4.3
3	4.9	5.5	5.0	— 6.8	872	197	— 3.6
4	6.3	6.4	6.1	— 7.6	818	210	— 3.5
5	6.0	7.2	7.4	— 6.4	995	207	— 4.4
6	5.0	6.6	6.6	— 5.8	878	209	— 3.9
7	5.8	6.0	6.1	— 7.4	975	198	— 4.3
8	5.0	6.8	6.8	— 5.6	747	221	— 3.6
9	5.0	6.9	6.8	— 5.5	812	211	— 3.0
10	5.1	4.9	5.0	— 7.6	597	221	— 3.4
11	9.1	11.2	10.5	— 7.5	2400	160	— 6.8
12	9.5	12.2	11.5	— 7.3	2241	175	— 6.8
13	9.0	10.9	11.2	— 7.6	2848	147	— 8.6
14	12.0	17.7	14.0	— 7.6	7718	51	— 14.2

Remarks

[1]) Defined by eq. [3] estimated max. error $\pm$ 0.5.
[2]) Viscosity (P) at 20 °C from master curve estimated max. error $\pm$ 0.3.
[3]) Viscosity (P) at 20 °C extrapolated from viscosity measurements at higher temperatures estimated max. error $\pm$ 0.3.
[4])Defined by eq. [3] evaluated from 3rd col. of this table by eq. [5] using log $G_g = 9.7$; dimension: seconds estimated max. error $\pm$ 1.0.
[5]) Defined by eq. [15], °K; for samples 1–10 estimated max. error $\pm$ 5%; for samples 11–14 estimated max. error $\pm$ 10%.
[6]) Defined by eq. [15], °K; for samples 1–10 estimated max. error $\pm$ 5 °K; for samples 11–14 estimated max. error $\pm$ 15 °K.
[7]) Defined by eq. [15], using 3rd col. estimated max. error $\pm$ 0.3.

in table 2 that τ_m varies much less than the viscosities at 20 °C, indicating that the latter – for the present set of samples – are largely governed by the width of the relaxation spectra.

The fact that the master curves of the bitumens can all be derived from log *Gaussian* spectra, which only vary in width, is certainly one of the reasons of the regularity to which we referred in the introduction. Furthermore, we may point to a peculiarity in the shapes of the master curves for various values of β. It was found numerically that the modulus values at constant phase angle with varying β are on a fan of straight lines in the double logarithmic plot of fig. 2.

The viscous flow and elastic deformation asymptotes form the extreme members of the fan. As an example we have drawn some lines of constant phase angle in fig. 2.

Log *Gaussian* relaxation time distributions have also been found in dielectrical (13) and mechanical relaxation (15) with simple liquids of which the molecules are associated by hydrogen bonding. Although bitumens are by no means simple liquids which can be discussed in terms of interactions between "the" molecules, it is plausible to attribute a bonding capacity to a fraction of the constituent molecules, viz. the "asphaltenes" and it is known that the interactions in this fraction are of a hydrogen bonding nature. The variation of type as seen by the increasing values of β from samples 1 to 14 is accompanied by increasing asphaltenes content. Since the variation of the spectrum with varying type only comes about as a change in spectrum width we tend to conclude that the effects of asphaltenes – and possibly also of other fractions which vary with changing type – contribute to the whole spectrum. This conclusion is at variance with a tentative discussion by *E. Thelen* (16) of the spectra published by *Brodnyan* (2). *Thelen* discusses a subdivision of the spectra in zones to which the various component fractions are believed to contribute specifically.

Recently it has been shown (10, 17) that for many pure liquids the plots of storage and loss moduli against relative frequency coincided if the moduli were taken relative to the (specific) glassy modulus of the liquids. The common modulus function could be described by a simple mathematical formula (17), which (from the initials of the authors) will be denoted as the B.E.L. model.

Very recently, the B.E.L. model has been provided with an adjustable constant K to fit the data for binary mixtures of pure liquids (18) and also *Hutton* and *Phillips* (19) needed an adjustable B.E.L. model to account for their results on heptamethylnonane.

In the upper part of fig. 5 we have plotted the curves for the original B.E.L. model ($K = 1$) and a set of curves obtained from a log normal distribution. The value of $\beta = 2.6$ was chosen to obtain equal moduli at a relative frequency of unity. We note that there is quite a close correspondence between the two models. For the choice $\beta = 2.6$ the maximum deviation is about 6% in G_1. As a consequence, we may note that our sample no. 1 ($\beta = 2.5$) behaves very much like the pure liquids studied by *Lamb* et al.

On the other hand, the behaviour of the bitumens characterized by higher β values increasingly departs from that of the (adjustable) B.E.L. model. The lower part of fig. 5 shows that the case $\beta = 5$ qualitatively corresponds with $K = 8$. This demonstrates the onset of a horizontal section at 45° in the phase angle curve, which effect becomes more pronounced at higher K values. These results show that the assumption of log normal relaxation spectra is more suitable for a general description of the relaxation behaviour of bitumens than the B.E.L. model.

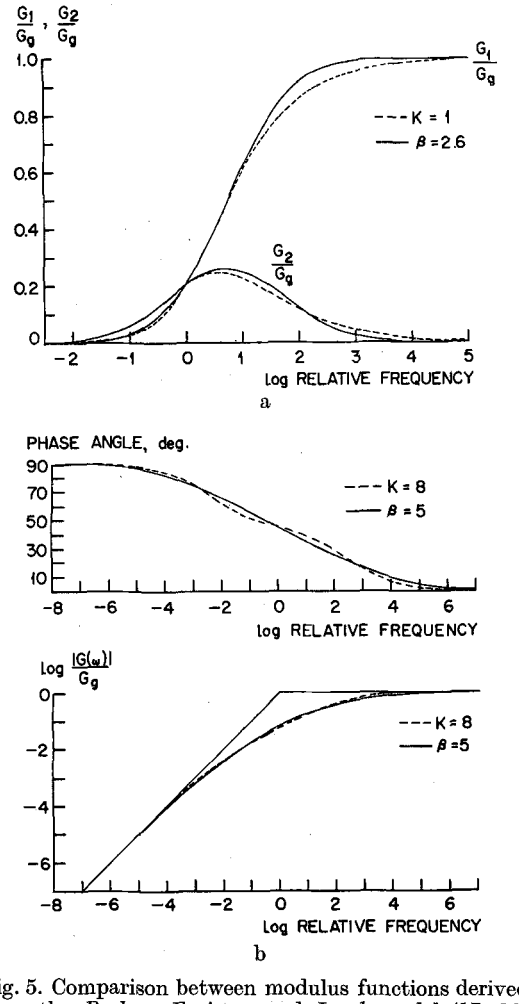

Fig. 5. Comparison between modulus functions derived from the *Barlow*, *Erginsav* and *Lamb* model (17, 18) and from log normal distributions of relaxation time

b) Viscosity-temperature functions

We took one of the measuring temperatures of each series as a reference temperature T_R (generally in the middle of the range covered) and determined the viscosity shifts with respect to it. The WLF constants C_1 and C_2, corresponding with T_R according to:

$$\log a_T = \log \frac{\eta_0(T)}{\eta_0(T_R)} = \frac{-C_1(T - T_R)}{C_2 + (T - T_R)} \qquad [11]$$

are evaluated from a plot of $-\frac{T - T_R}{\log a_T}$ versus $T - T_R$. From a rearrangement of eq. [11]:

$$-\frac{T - T_R}{\log a_T} = \frac{C_2}{C_1} + \frac{1}{C_1}(T - T_R) \qquad [12]$$

it can be seen that C_1 and C_2 can be obtained from the slope and intercept at $T = T_R$ of the straight-line portion of the above-mentioned plot.

The values of C_1 and C_2 obtained in this way are not worth mentioning unless T_R is chosen with a physical significance. Another way is to express the free-volume constants independent of the reference temperature by taking

$$C_1 \times C_2 = B \quad \text{and} \quad T_R - C_2 = T_0 \qquad [14]$$

in which B and T_0 are constants in the *Vogel* eq. [20]

$$\log \eta = A + \frac{B}{T - T_0}. \qquad [15]$$

The values of B and T_0 and of the adjustment factor A are collected in table 2. Eq. [11] and eq. [15] gave a reasonable description of the average frequency-temperature shifts for the rubbery samples, but for the pitch and road-type bitumens considerable deviations were found at the lowest temperatures. This is demonstrated in fig. 3, in which the lines correspond with eq. [15] for the parameter values in table 2.

The deviations are evidently not a function of the viscosity or of the temperature and, as can be inferred from table 1, neither of the difference between measuring temperature and glass-transition temperature, although for the road and pitch-type bitumens the deviations start at about

50 °C above T_g. We think that the deviations are caused by non-validity of eq. [15] at too low values of $T - T_0$.

Such a non-validity is evident, since free volume will not exactly be zero for $T < T_0$ and proportional to $T - T_0$ for $T > T_0$. We tried to replace the numerator of eq. [15] by a function which "tails off" below $T = T_0$ rather than becoming zero for $T < T_0$. With the hyperbolic form $g_h(T - T_0)$ for which $g(T - T_0) = T - T_0$ is an asymptote as a numerator in eq. [15]:

$$g_h(T - T_0) = \frac{1}{2}\{T - T_0 + \sqrt{(T - T_0)^2 + C}\} \quad [16]$$

we could find values for A, B, C and T_0 which gave a good fit over the entire range. The full line in fig. 3 gives the results on sample no. 1 for the values $A = -4.6$, $B = 800$, $T_0 = 225$ and $C = 2350$. This method is not further discussed, since many other four parameter equations would fit and there is no a priori justification of eq. [16]. We neither expect success from the addition of an *Arrhenius* term to eq. [15], since the results at higher temperatures are well described by the free-volume equations.

Accepting the limited validity of eq. [11] and [15] – which limits are by no means narrow – we may now discuss the values of B and T_0 obtained. It can be seen from table 2 that on the average high values of B are associated with low values of T_0 and vice versa. Although B and T_0 cannot be determined completely independently, the variation of B with T_0 appears to be significant. A similar relation between the two *Vogel* constants is found in the results in table 1 of ref. 17.

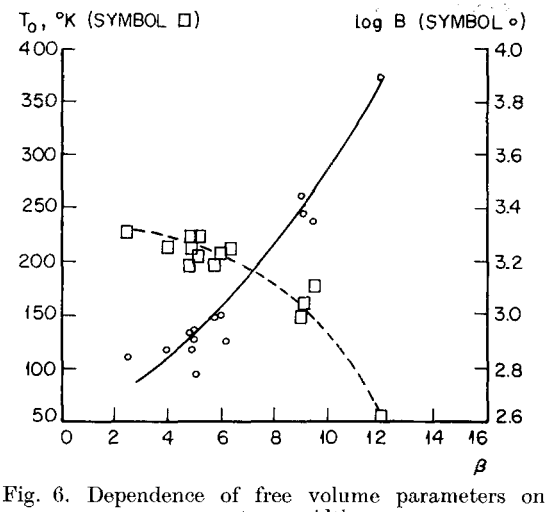

Fig. 6. Dependence of free volume parameters on spectrum width

Fig. 6 shows that the free-volume constants B and T_0 depend on the type of bitumen if the latter is expressed by β.

The fact that B varies with the type of bitumen implies (eq. [14]) that it is impossible to assign to each material a specific reference temperature which yields a common pair of WLF constants for all bitumens. Nevertheless, the B values of the road and pitch bitumens are close to the value of 900, associated with the "universal" WLF constants $C_1 = 8.86$ and $C_2 = 101.6$.

If we plot the two WLF constants, obtained by taking the glass-transition temperatures as a reference (fig. 7a), we see that the result is not one set, i. e. one point in fig. 7a,

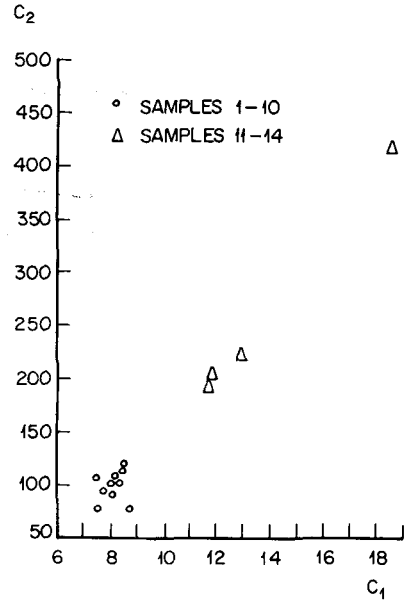

Fig. 7a. WLF constants with glass-transition temperature as a reference

but two groups. One group corresponds with β values below 6 and the rest with higher β values. An interesting figure is obtained when an equiviscous temperature is taken as a reference.

Fig. 7b shows the results for an equiviscous temperature of 2×10^4 P. This gives a more regular picture, in which the three groups of bitumens are "in line". A similar picture is obtained with other equiviscous temperatures. As a consequence of the difference between fig. 7a and b we may conclude that T_g is not an equiviscous temperature for our samples.

If the difference between the coefficients of expansion in the liquid and the glassy state is taken as the coefficient of expansion of free volume, we can calculate the free

volume fraction f_g at T_g. The values are given in table 1, and illustrate that T_g is not an equi-free-volume temperature for our results either. One may doubt the values obtained from T_g by volume dilatometry, since the transition is not very sharp – the region from T_a to T_b in fig. 4 is generally of the order of 30 °C – and there is an uncertainty of about 3 °C in the values due to some arbitrariness in choice of the lines a and b in fig. 4. Nevertheless, good correlation has been observed between results from dilatometry and differential thermal analysis (21), so that the experimental uncertainty in T_g is probably not very large.

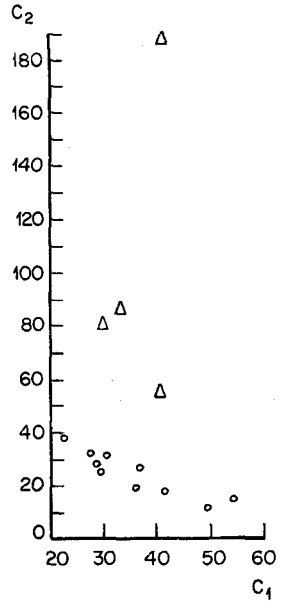

Fig. 7b. WLF constants with equiviscous temperature of 2×10^4 P as a reference

The uncertainty seems rather to be on the phenomenological side, in that T_g only defines corresponding states between samples of the same type – with the same shear relaxation and volume relaxation time distributions.

A reason for the failure of a corresponding states principle on the basis of T_g for varying types of bitumen is perhaps that we try to correlate the equilibrium free volume fractions as a function of temperature (from e. g. viscosities) with a non-equilibrium measurement of free volume.

The effect of cooling rate is small in our view: T_g changed less than 3 °C with samples 6 and 14 for cooling rates varying from 0.3 to 3.0 °C/min. Nevertheless, much larger differences in T_g might have been observed if the cooling rates had been chosen in such a way that for each sample the same approach to equilibrium was ensured.

The influence of the type of sample on the significance of T_g is most clearly illustrated by the fact that the dilatometric glass-transition temperatures approach the "thermodynamic glass-transition temperatures" T_0 as the spectrum becomes narrower, i. e. as β decreases.

Summary

Thermorheological behaviour and dilatometric glass-transition temperatures have been studied on 14 samples representing the three main types of bitumen. The frequency dependence of the dynamic moduli can be described by *Gaussian* distributions of log relaxation time. The width of the distribution depends on the type of bitumen.

The frequency-temperature shifts or the viscosity-temperature relations correspond with free-volume equations for temperatures not too close to the thermodynamic glass-transition temperatures. The constants in the free-volume equations vary with the type of bitumen.

The dilatometric glass-transition temperatures do not serve as simple references for corresponding free volume states. Their significance was found to depend on the type of bitumen. In this respect it is noteworthy that the dilatometric glass-transition temperatures approach the thermodynamic ones as the spectra become narrower.

Zusammenfassung

Das thermorheologische Verhalten und die dilatometrischen Glasübergangstemperaturen von Bitumen wurden an 14 für die drei Haupttypen charakteristischen Proben untersucht. Die Frequenzabhängigkeit läßt sich durch Gauß-Verteilungen der log. Relaxationszeit beschreiben. Die Verteilungsbreite ist durch den Bitumentyp bedingt.

Die Frequenz–Temperatur-Verschiebungen bzw. die Viskositäts–Temperatur-Beziehungen entsprechen Gleichungen vom Typ des freien Volumens für Temperaturen, die nicht zu nahe den thermodynamischen Glasübergangstemperaturen liegen. Die Konstanten in diesen Gleichungen ändern sich mit dem Bitumentyp.

Die dilatometrischen Glasübergangstemperaturen können nicht als einfache Vergleichstemperaturen für entsprechende Zustände des freien Volumens dienen. Es wird gezeigt, daß ihre Bedeutung vom Bitumentyp abhängig ist. In diesem Zusammenhang ist zu bemerken, daß sich die dilatometrischen Glasübergangstemperaturen den thermodynamischen mit schmaler werdenden Spektren nähern.

References

1) *Van der Poel, C.*, J. Appl. Chem. (London) **4**, 221 (1954).

2) *Brodnyan, J. G.*, Highway Res. Bull. **192**, 1 (1958).

3) *Wada, Y.* and *H. Hirose*, J. Phys. Soc. Japan **15**, 1885 (1960).

4) *Schmidt, R. J.* and *L. E. Santucci*, Proc. AAPT **35**, 61 (1966).

5) ASTM Method D 2170–67.

6) *Labout, J. W. A.*, Rheol. Acta **1**, 186 (1958).

7) *Schmidt, R. J., R. F. Boynton* and *L. E. Santucci*, ACS Preprints **10**, 17 (1965).

8) *Schwarzl, F.* and *A. J. Staverman*, J. Appl. Phys. **23**, 838 (1952).
9) *Ferry, J. D.*, Viscoelastic properties of polymers, p. 209 (New York 1961).
10) *Barlow, A. J., J. Lamb, A. J. Matheson, P. R. K. L. Padmini* and *J. Richter*, Proc. Roy. Soc. A **298**, 467 (1967).
11) *Saal, R. N.*, (unpublished work).
12) *Ninomya, K.* and *J. D. Ferry*, J. Colloid Sci. **14**, 36 (1959).
13) *Yager, W. A.*, Physics **7**, 434 (1936).
14) *Nowick, A. S.* and *B. T. Berry*, IBM J. Res. Develop. **5**, 297 (1961).
15) *Litovitz, T. A.* and *C. M. Davies*, Physical Acoustics *W. P. Mason* ed., Vol. 2, part A, Ch. 4, p. 281 (New York 1965).
16) *Thelen, E.*, Repr. Amer. Chem. Soc. Div. Petr., **9**, no. 2, B–5 (1964).
17) *Barlow, A. J., A. Erginsav* and *J. Lamb*, Proc. Roy. Soc. A **298**, 481 (1967).
18) *Harrison, G.* and *J. Lamb*, Rheology Abstr. **11**, 146 (1968).
19) *Hutton, J. F.* and *M. C. Phillips*, Rheology Abstr. **11**, 145 (1968).
20) *Vogel, H.*, Physik. Z. **22**, 645 (1921).
21) *Connor, H. J.* and *J. G. Spiro*, J. Inst. Petrol. **54**, 137 (1968).

Authors' address:
Ir. *R. Jongepier* and *B. Kuilman*
Koninklijke Shell Laboratorium Shell Research N. V.
Amsterdam (Netherlands)

From the Royal Military College of Science, Shrivenham (U. K.)

Fatigue crack growth studies on constant compliance specimen

By N. J. I. Adams

With 6 figures in 7 details and 2 tables

(Received January 18, 1969)

Symbols:

a	crack length, ins.
a_0	initial crack length
c	constant
e	distance from wedge tip to line of load application, ins.
H_p	depth of tapered split arm at load line ins.
K_I	stress intensity p.s.i. $\sqrt{\text{ins}}$
$K_{If\max}$	maximum fatigue stress intensity p.s.i. $\sqrt{\text{ins}}$
$K_{If\min}$	minimum fatigue stress intensity p.s.i. $\sqrt{\text{ins}}$
N	number of cycles
P	load. lb.
R	stress intensity ratio < 1.
σ	stress p.s.i.

Introduction

The study of problems of fatigue crack growth has in the past been conducted on wide centre-cracked plates [1, 2]. The crack is grown from an initial starter notch, and as it extends so the crack tip conditions vary continuously. Such specimens require complex end fittings and high load capacity testing machines. The constant compliance specimen is a small compact form suggested for fracture toughness testing. It has the property of constant crack tip stress intensity for non-dimensional crack lengths a/W, approximately equal to 0.25 to 0.5 and requires only a low load capacity machine for testing.

Specimen configuration and experimental set-up

Fig. 1 shows the details of the specimen used in the work which is reported. The dimensions are based on a quarter crack length to suit available crack growth recording gauges and the K_I calibration by (3) which gives

$$\frac{K_I B W^{1/2}}{P} = 14.2$$

for

$$\frac{H_p}{e} = 0.4, \quad \frac{W}{e} = 5 \quad \text{and} \quad \frac{W}{H_p} = 12.5.$$

It was pointed out in (3) that forward direction crack growth was highly unstable and to overcome

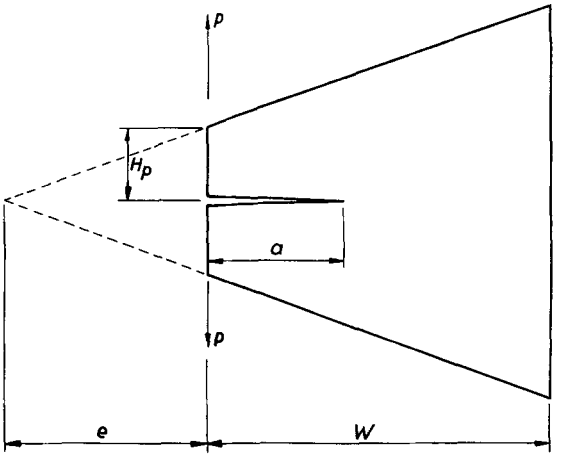

Fig. 1a. Geometry of constant compliance specimen